

Support Information

Facile preparation of copper based amorphous/crystalline heterophase nanocatalysts and their applications as efficient non-enzymatic biosensors

Ruopeng Zhao,^{a,b} Xiaonan Shi,^{a,b} Jing Liu,^{a,b} Peiyang Zhou,^{a,b} Yandi Zhou,^{a,b} Zhangyong Wu,^{a,b} Lin Yao,^{a,b} Yong Liu,^{*a,b} and Changrong Zhao^{*c}

^aLaboratory of Novel Optoelectronic Technology for Ophthalmic **Devices** (NOTOD), School of Ophthalmology and Optometry, School of Biomedical Engineering, Wenzhou Medical University, Wenzhou, 325027, PR China.

^bNational Engineering Research Center of Ophthalmology and Optometry, Eye Hospital, Wenzhou Medical University, Wenzhou, 325027, China.

^cSchool of Laboratory Medicine and Life Sciences, Wenzhou Medical University, Wenzhou, 325027, PR China.

Corresponding emails: yongliu@wmu.edu.cn and crzhao8017@163.com

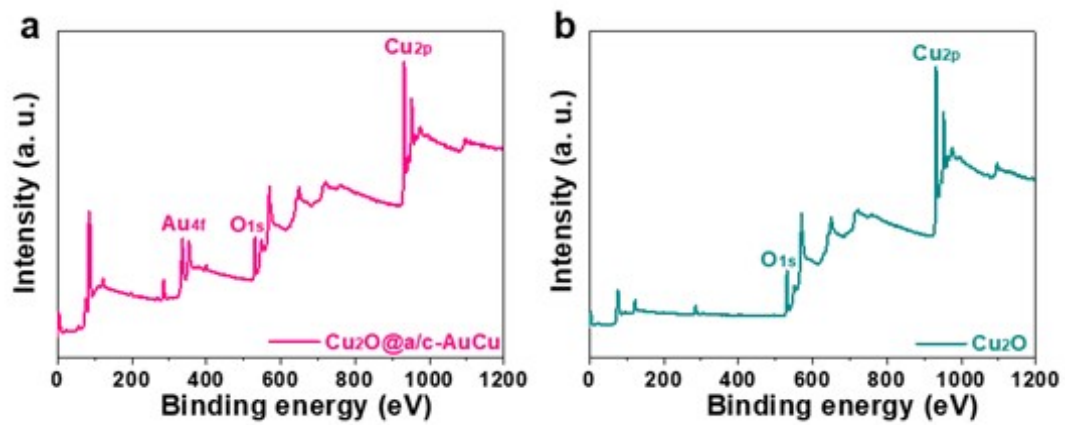


Figure S1. The XPS spectrum of (a) $\text{Cu}_2\text{O}@a/c\text{-AuCu}$, and (b) Cu_2O .

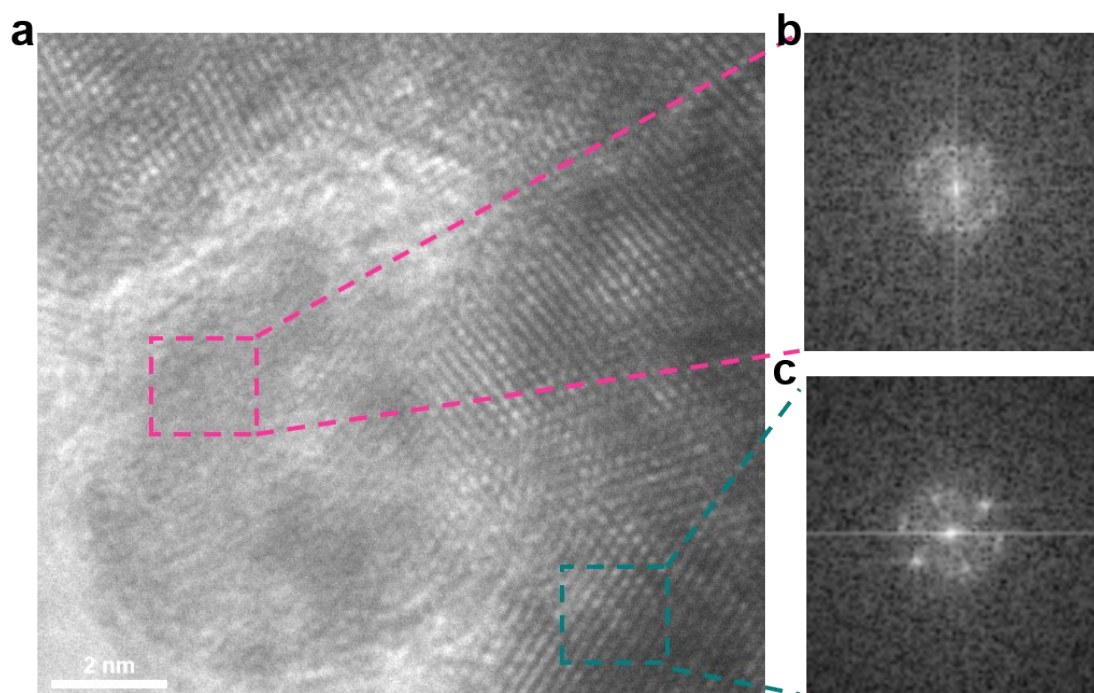


Figure S2. (a) High-resolution TEM image of the $\text{Cu}_2\text{O}@a/c\text{-AuCu}$ alloy; (b) & (c) the corresponding fast Fourier transform (FFT) patterns from the different selected regions of (a).

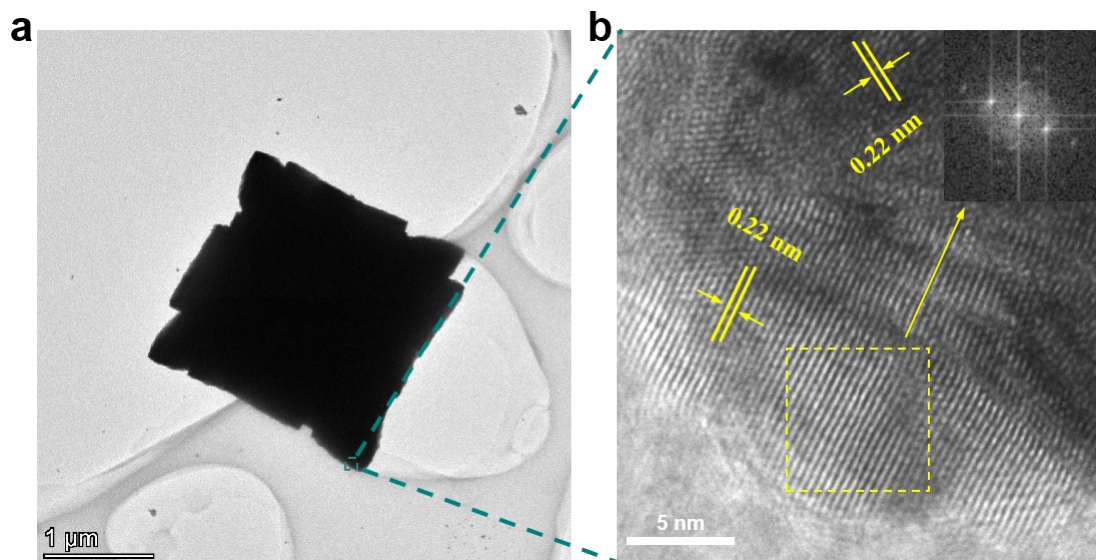


Figure S3. (a) TEM image and (b) High-resolution TEM image of the $\text{Cu}_2\text{O}@c\text{-AuCu}$ alloy. Insert of (b): the corresponding fast Fourier transform (FFT) patterns of the selected yellow region.

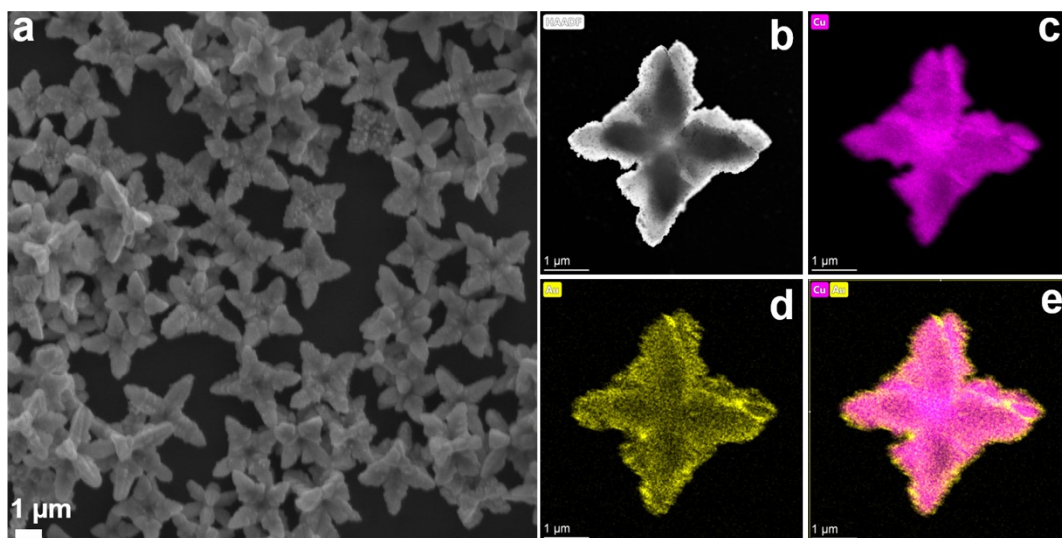


Figure S4. (a) SEM image and (b-e) element mapping images of the $\text{Cu}_2\text{O}@c\text{-AuCu}$ alloy.

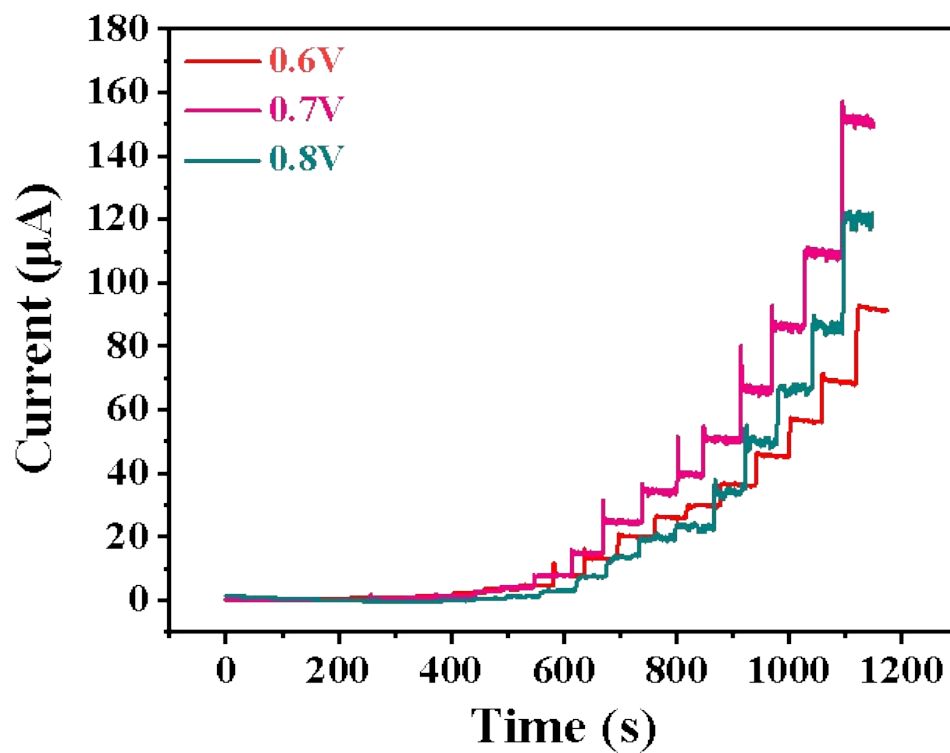


Figure S5. The chronoamperometry measurements polarized at different potentials after the continuous addition of glucose into 0.1 M NaOH solution.

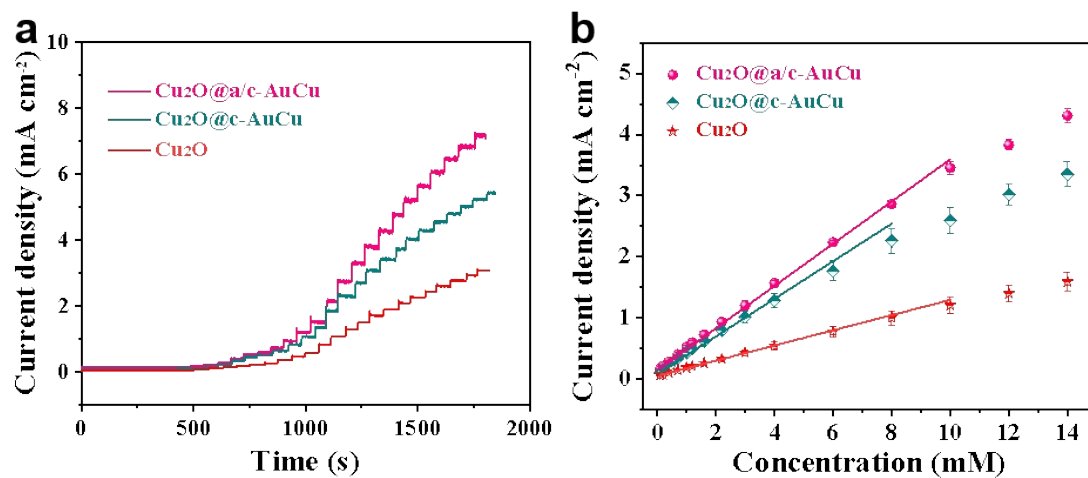


Figure S6. (a) The sensing performance of different sensors after the continuous addition of glucose at 0.7 V; (b) the corresponding calibration curves.

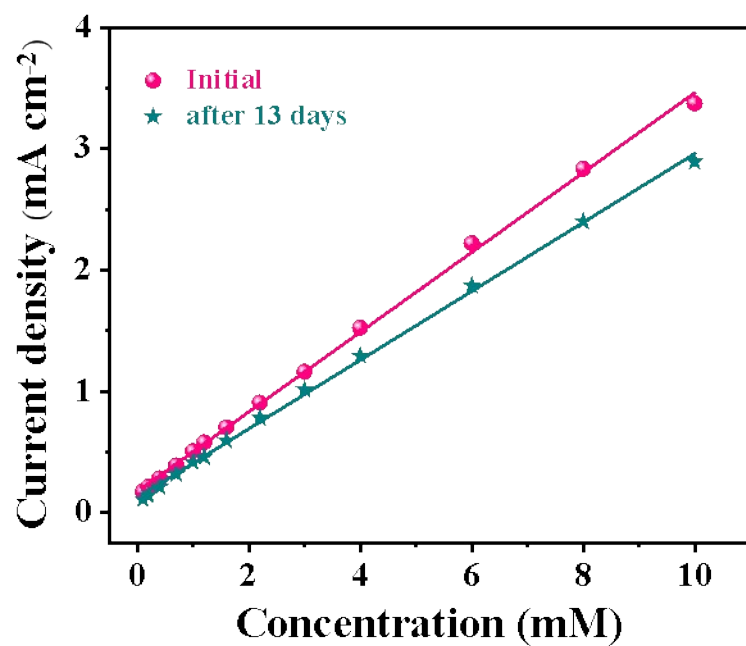


Figure S7. The corresponding calibration curves obtained from the long-term sensing stability test.

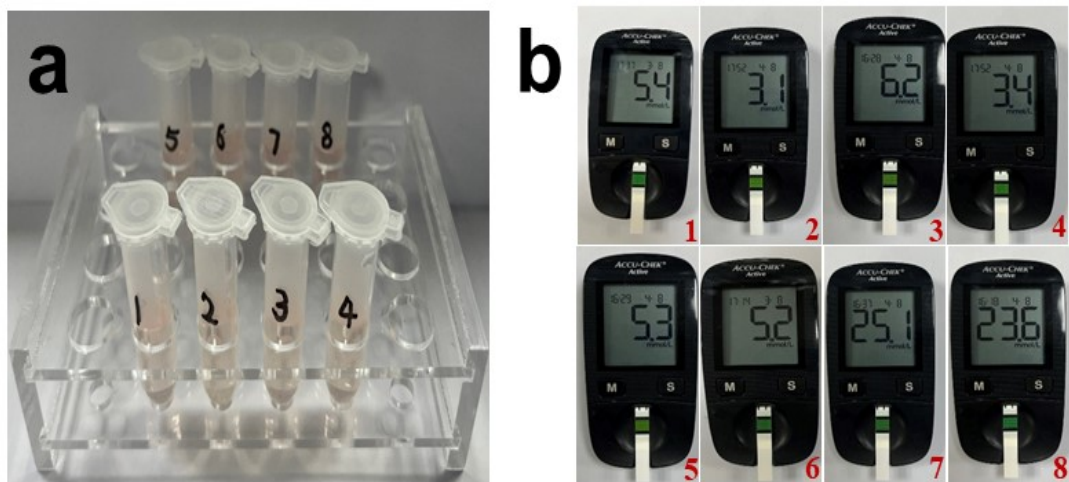


Figure S8. (a) Digital photos of the **rat** serum samples; and (b) the glucose testing results using the commercial **glucometer**.

Table S1. The glucose detection performance of the Cu₂O@a/c-AuCu sensor compared to the other reported non-enzymatic sensors.

No.	Catalysts	Linear range (mM)	Sensitivity ($\mu\text{A mM}^{-1} \text{cm}^{-2}$)	Detection Limit (μM)	Ref
1	Pt@Pd nanoparticles	0.01-9.2	247.3	3	1
2	PtCu Nanochains	0.01-17	135	2.5	2
3	Cu@Cu ₂ O	0.001-17.12	194.88	0.6	3
4	Cu ₂ O SLNs	0.01-2.97	0.933	0.035	4
5	CuO/g-C ₃ N ₄	0.0005-8.5	274	0.15	5
6	Ag-CuO/rGO	0.01-28	214.37	0.76	6
7	Cu ₂ O nanocubes	0.3-3.3	285	3.3	7
8	Cu ₂ O@a/c-AuCu alloy	0.1-10	345	1.35	This work

Table S2. Detection and recovery of glucose in **rat** serums.

Sample	Added (μM)	Found (μM)	Recovery	RSD (n=3)
1	10.00	11.40	114.05%	3.30%
2	10.00	11.20	112.00%	1.81%
3	10.00	9.20	91.76%	8.34%

Reference

1. M. A. Zahed, S. C. Barman, P. S. Das, M. Sharifuzzaman, H. S. Yoon, S. H. Yoon and J. Y. Park, *Biosens. Bioelectron.*, 2020, **160**, 112220.
2. X. Cao, N. Wang, S. Jia and Y. Shao, *Anal. Chem.*, 2013, **85**, 5040-5046.
3. Y. Gao, F. Yang, Q. Yu, R. Fan, M. Yang, S. Rao, Q. Lan, Z. Yang and Z. Yang, *Microchim. Acta*, 2019, **186**, 1-9.
4. R. Khan, R. Ahmad, P. Rai, L.-W. Jang, J.-H. Yun, Y.-T. Yu, Y.-B. Hahn and I.-H. Lee, *Sensor Actuat B-Chem*, 2014, **203**, 471-476.
5. Y. Huang, Y. Tan, C. Feng, S. Wang, H. Wu and G. Zhang, *Microchim. Acta*, 2019, **186**, 1-9.
6. D. Xu, C. Zhu, X. Meng, Z. Chen, Y. Li, D. Zhang and S. Zhu, *Sensor Actuat B-Chem*, 2018, **265**, 435-442.
7. M. Liu, R. Liu and W. Chen, *Biosens. Bioelectron.*, 2013, **45**, 206.